

SrRuO₃/SrTiO₃/SrRuO₃ heterostructures for magnetic tunnel junctions

G. Herranz,^{a)} B. Martínez, and J. Fontcuberta

Institut de Ciència de Materials de Barcelona, Campus U.A.B. Bellaterra 08193, Catalunya, Spain

F. Sánchez, M. V. García-Cuëca, C. Ferrater, and M. Varela

Departament de Física Aplicada i Òptica, Universitat de Barcelona, Diagonal 647, Barcelona 08028, Catalunya, Spain

(Presented on 14 November 2002)

We report on the growth and characterization of SrRuO₃ single layers and SrRuO₃/SrTiO₃/SrRuO₃ heterostructures grown on SrTiO₃(100) substrates. The thickness dependence of the coercivity was determined for these single layers. Heterostructures with barrier thickness $t_b = 1, 2.5,$ and 4 nm were fabricated, with electrodes having thickness ranging from 10 to 100 nm. The hysteresis loops of heterostructures with $t_b = 2.5$ nm, 4 nm reveal uncoupled magnetic switching of the electrodes. Therefore, these heterostructures can be used for the fabrication of magnetic tunneling junctions.

© 2003 American Institute of Physics. [DOI: 10.1063/1.1555372]

Considerable efforts are focused on the research on magnetic tunnel junctions (MTJ), since they constitute an important alternative for higher density MRAMs and other spin devices.^{1,2} In order to build these junctions, heterostructures involving two ferromagnetic electrodes separated by an insulating nonmagnetic barrier must be grown. With the aim of having functional tunnel junctions, the magnetic electrodes must be magnetically uncoupled, i.e., they must rotate at different fields, so that the switch between parallel and anti-parallel alignments of the electrode magnetizations is allowed. This feature must be reflected in different coercivities for the two electrodes, hence a control of the coercive field is needed.

Certainly La_{1-x}Sr_xMnO₃ ferromagnetic electrodes offer substantial advantages due to their full spin polarization. However, they suffer a serious drawback: its response is very disappointing as the magnetoresistance of manganite-based MTJ decays very fast with temperature and becomes negligible well below the Curie temperature (T_C).^{3,4} It is believed that the nature of the ferromagnetic coupling in these oxides (double exchange), being extremely sensitive to the bond's topology and thus structural defects and interfaces, is at the heart of the rather poor response at high temperature. Therefore the use of SrRuO₃ (SRO) which is an itinerant ferromagnet⁵⁻⁷ with a negative spin polarization ($P = -9.5\%$) when measured by tunnel experiments with a SrTiO₃ barrier⁸ may have some advantages compared to those based in manganites, when used in the fabrication of MTJ. In this article we report on the growth and characterization of SRO single layers and SrRuO₃/SrTiO₃/SrRuO₃ (SRO/STO/SRO) heterostructures with the aim of being used in MTJ. First, we will show that film coercivity can be controlled by the thickness of the SRO film. This information will be used to grow uncoupled SRO/STO/SRO trilayers of different thickness.

The SRO films and the SRO/STO/SRO trilayers were grown on SrTiO₃(100) substrates by pulsed laser deposition (PLD) with a KrF excimer laser of $\lambda = 248$ nm at a repetition rate of 3 Hz. The bulk cell parameters of SRO and STO are 0.393 (pseudocubic) and 0.3905 nm, respectively, thus the structural mismatch is about 0.64%. The SrRuO₃ electrodes were grown with an oxygen pressure of 0.1 mbar, while the insulating SrTiO₃ barrier of thickness $t_b = 1, 2.5,$ and 4 nm were grown in an oxygen pressure of 10^{-3} mbar. The substrate remained throughout the growth of the heterostructures at a temperature of 675 °C. Oxygen pressure was progressively increased after switching off the laser, while the substrate was cooled down, in order to avoid any possible loss of oxygen.

Prior to the fabrication of these heterostructures, epitaxial SRO/SrTiO₃(100) films of various thicknesses ($t = 4-320$ nm) were grown using similar processing conditions. X-ray characterization,⁹ including $\theta-2\theta$, φ scans and reciprocal maps, revealed that the films are fully strained for all thicknesses reported here. This is achieved by the relatively small lattice parameter mismatch and the chosen growth conditions. In addition, these samples were fully characterized by magnetic and electrical transport measurements. The resistivity-temperature curves ($\rho-T$) show a well-defined kink associated to the onset of ferromagnetic order. This feature determines accurately the Curie temperature by plotting $d\rho/dT$ curves and locating the peak appearing at the transition temperature (Fig. 1 inset). Thus, we obtain values of the Curie temperature $T_C \geq 130$ K for films with thickness $t > 10$ nm. Furthermore, the films have room temperature resistivities in the range 200–400 $\mu\Omega$ cm, and a residual resistivity (at 4 K) of 80–100 $\mu\Omega$ cm.

Magnetic measurements performed on the 320 nm thick film (not shown), reveal that the easy direction of magnetization lies in an out-of-plane direction. Even in the thinner films, the demagnetizing field is far smaller than the anisotropy field, since $4\pi M_S \approx 2.5$ kOe, and values exceeding 20

^{a)}Electronic mail: gherranz@icmab.es

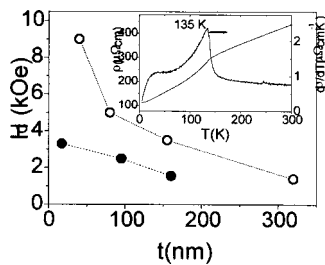


FIG. 1. Coercive field of SRO single layers at 5 K as a function of thickness for fields applied perpendicularly (●) and along (○) the plane of the films. Inset: Resistivity (ρ) of a SRO single layer as a function of the temperature, together with $d\rho/dT$. The peak appearing in the latter is used to track the Curie temperature.

kOe are reported for the anisotropy field.^{10,11} Thus, it can be expected that the easy axis of magnetization lies in the out-of-plane direction for any value of thickness. In fact, Izumi *et al.* reported a uniaxial out-of-plane magnetic anisotropy for an ~ 1 nm thick SRO film in SRO/STO superlattices.¹² Hysteresis loops at low temperature (5 K) have been measured for SRO single layer films of different thickness with the magnetic field applied both within the plane of the film and normal to it. The experimental data are included in Fig. 1, from which the coercive field (H_C) is determined. As expected, a similar thickness dependence of H_C is observed for both field orientations. This dependence was already found in some previous reports.^{12–14} It follows from data in Fig. 1 that we can control the coercive fields of the ferromagnetic electrodes through the thickness.

In order to build the SRO/STO/SRO heterostructure, the first step is to grow the STO insulating layer on top of the bottom SRO electrode. In what follows we shall restrict our description of results to those obtained using bottom electrodes around 90 nm thick. To have operative tunnel junctions it is of fundamental importance to know the surface structure of the insulating layer. With this purpose we have collected atomic force microscopy (AFM) images of a STO barrier of $t_b = 4$ nm grown on a SRO(88 nm) layer. Figure 2(a) shows that the original structure of terraces and steps of the SRO single layer¹⁵ is also visible on the STO surface. The averaged roughness (rms) is ~ 0.5 nm on a $5 \times 5 \mu\text{m}$ area. As illustrated by the line scan shown in Fig. 2(b), steps of two unit cells are commonly observed, separating terraces of about 100 nm wide. Detailed inspection of the AFM images shows the presence of 2D (up to two unit cells high) islands, most of them close to the steps, although there are other in the middle of the terraces. Island density, size, and space distribution suggests that the first growth mechanism is nucleation at step edges of the underlying SRO/STO structure. This observation is consistent with previous reports of SRO growth on STO miscut substrates.¹⁶

From the above analysis it appears that the STO barrier is of good quality and flat enough to be used as an insulating barrier in a SRO/STO/SRO structure. Notice that the height of steps and islands, as well as the depth of a few holes that were observed, are below 1 nm. Consequently, the 4 nm thick STO layer is expected to be able to uncouple electrically and magnetically the SRO electrodes.

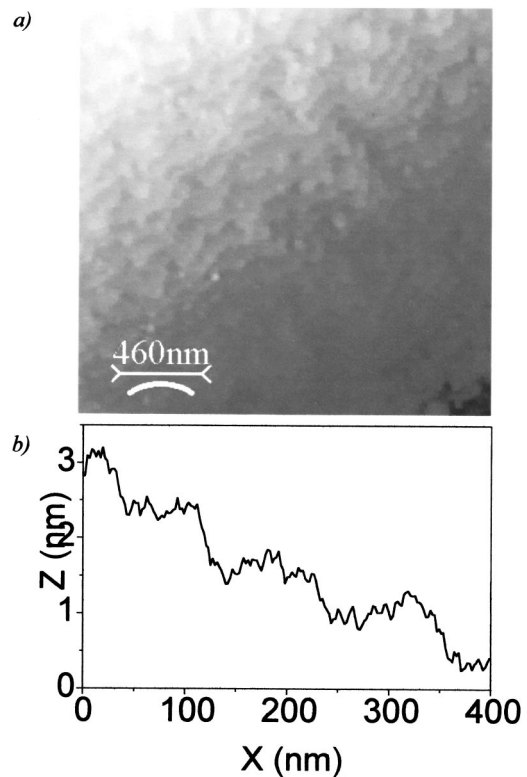


FIG. 2. (a) Top view image of the surface morphology of a bilayer STO (4 nm)/SRO (88 nm); (b) profile taken across the steps appearing in the previous image, showing that the steps are two units cell high.

In Fig. 3 we plot the magnetization versus temperature $M(T)$ for both a trilayer SRO(14 nm)/STO(4 nm)/SRO(100 nm) and the bilayer STO(4 nm)/SRO(88 nm). In agreement with the above discussion, and with the purpose of having the smaller possible values for the switching fields, the external magnetic field in these measurements has been applied perpendicularly to the film plane. We first note (see inset in Fig. 3) that the Curie temperature of the bilayer is $T_C \approx 123$ K and that of the trilayer is $T_C \approx 110$ K. These T_C values are somewhat lower than those routinely obtained in single SRO layers (> 130 K). This observation suggests that, very likely, during the growth of the STO barrier—done at a lower pressure than that of the SRO electrodes—there is

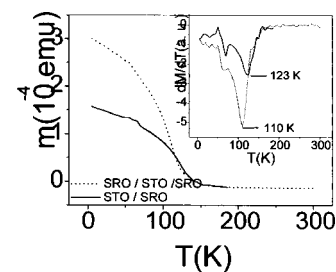


FIG. 3. Plot of the magnetization (m) vs temperature for both a SrRuO₃ (14 nm)/SrTiO₃ (4 nm)/SrRuO₃ (100 nm) (SRO/STO/SRO) and a SrTiO₃ (4 nm)/SrRuO₃ (88 nm) (STO/SRO) heterostructures (with an applied field of 5000 Oe normal to the heterostructure). Inset: The transition temperatures, determined through locating the peaks in the dM/dT curves, are indicated in this plot.

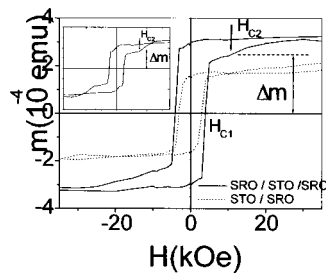


FIG. 4. Hysteresis loops for the SRO(14 nm)/STO(4 nm)/SRO(100 nm) heterostructure and the STO(4 nm)/SRO(88 nm) heterostructure. The two coercive fields are indicated. The magnetization jump corresponding to the lower coercive field is also indicated. Inset: Hysteresis loop corresponding to a SRO(9 nm)/STO(2.5 nm)/SRO(68 nm) heterostructure. All the measurements were performed at 5 K.

some oxygen loss in the SRO layers that reverts in a drop of the corresponding T_C .

In Fig. 4 hysteresis loops of the studied heterostructures, with the field applied perpendicular to the plane, are plotted. For the SRO(14 nm)/STO(4 nm)/SRO(100 nm) trilayer we observe two different coercive fields $H_{C1} \approx 4$ kOe and $H_{C2} \approx 10$ kOe, corresponding to the magnetization reversal of each electrode. We should also stress that the jumps in magnetization associated with each coercive field are, within experimental error, consistent with the electrodes being uniformly magnetized, each with its own thickness. As seen in Fig. 4, the jump in magnetization related to the lower coercive field is $\Delta m \approx 2.5 \times 10^{-4}$ emu, whereas the full magnetization of the whole heterostructure is about $m_s \approx 3.2 \times 10^{-4}$ emu. Assuming a uniform magnetization in each electrode, we find that the ratio $\Delta m/m_s \approx 0.78$, whereas the ratio between the nominal thickness of the bottom electrode (100 nm) and the nominal whole electrode thickness is about 0.88. Thus, within this experimental error, the previous remarks suggest that the magnetization of each electrode rotates independently. A similar analysis can be applied to the SRO(9 nm)/STO(2.5 nm)/SRO(68 nm) heterostructure, whose hysteresis loop is shown in the inset of the Fig. 4. Here $\Delta m/m_s \approx 0.67$ and the ratio corresponding to the nominal thickness values is about 0.88. In passing we mention that the magnetic saturation M_S has a value of $1.3 \mu_B/f.u.$,

in agreement with the reported values of M_S , confirming the good quality of the films.

In summary, we have been able to grow SrTiO₃/SrRuO₃/SrTiO₃ heterostructures with magnetically uncoupled electrodes, thus opening the way to their use for the fabrication of magnetic tunneling junctions. We can control the coercivities of the electrodes by setting their thickness. Therefore, we can switch from parallel to antiparallel alignment of the electrode magnetizations by sweeping the applied magnetic field. After submission of this manuscript we have known that recently Choi *et al.* have reported fabrication of MTJs based on SRO/STO/SRO structures.¹⁷

Financial support by the CICYT (MAT99-0984-C03 and MAT2000-1290-C03-03) and the Generalitat de Catalunya (GRQ99-8029) are acknowledged. This work is dedicated to Professor Domingo González from the University of Zaragoza, on the occasion of his retirement.

- ¹G. A. Prinz, *J. Magn. Magn. Mater.* **200**, 57 (1999).
- ²J. S. Moodera and G. Mathon, *J. Magn. Magn. Mater.* **200**, 248 (1999).
- ³A. Gupta and J. Z. Sun, *J. Magn. Magn. Mater.* **200**, 24 (1999).
- ⁴J. M. D. Coey, M. Viret, and S. von Molnár, *Adv. Phys.* **48**, 167 (1999).
- ⁵P. B. Allen, H. Berger, O. Chauvet, L. Forro, T. Jarlborg, A. Junod, B. Revaz, and G. Santi, *Phys. Rev. B* **53**, 4393 (1996).
- ⁶I. I. Mazin and D. J. Singh, *Phys. Rev. B* **56**, 2356 (1997).
- ⁷G. Cao, S. McCall, M. Shepard, J. E. Crow, and R. P. Guertin, *Phys. Rev. B* **56**, 321 (1997).
- ⁸D. C. Worledge and T. H. Geballe, *Phys. Rev. Lett.* **85**, 5182 (2000).
- ⁹G. Herranz, F. Sánchez, M. V. García-Cuenca, C. Ferrater, M. Varela, B. Martínez, and J. Fontcuberta, *Mater. Res. Soc. Symp. Proc.* **690**, 43 (2002).
- ¹⁰A. Kanbayasi, *J. Phys. Soc. Jpn.* **41**, 1879 (1976).
- ¹¹L. Klein, J. S. Dodge, C. H. Ahn, J. W. Reiner, L. Mieville, T. H. Geballe, M. R. Beasley, and A. Kapitulnik, *J. Phys.: Condens. Matter* **8**, 10111 (1996).
- ¹²M. Izumi, K. Nakazawa, Y. Bando, Y. Yoneda, and H. Terauchi, *Solid State Ionics* **108**, 227 (1998).
- ¹³M. Izumi, K. Nakazawa, Y. Bando, and Y. Yoneda, *J. Phys. Soc. Jpn.* **66**, 3893 (1997).
- ¹⁴S. C. Gausepohl, M. Lee, K. Char, R. A. Rao, and C. B. Eom, *Phys. Rev. B* **52**, 3459 (1995).
- ¹⁵G. Herranz, F. Sánchez, M. V. García-Cuenca, C. Ferrater, M. Varela, B. Martínez, and J. Fontcuberta, *Appl. Phys. Lett.* **82**, 85 (2003).
- ¹⁶J. Choi, C. B. Eom, G. Rijnders, H. Rogalla, and D. H. A. Blank, *Appl. Phys. Lett.* **79**, 1447 (2001).
- ¹⁷J. Choi, J. S. Noh, C. B. Eom, G. Rijnders, H. Rogalla, D. H. A. Blank, W. Tian, X. Q. Pan, H. C. Kim, H. Lee, and B. Oh, APS March Meeting 2002 (abstract).